Errors Caused by Long-Term Drifts of Magnetron Frequencies for Refractivity Measurement with a Radar: Theoretical Formulation and Initial Validation

JACQUES PARENT DU CHATELET

Météo-France, DSO, Toulouse, and LATMOS, Guyancourt, France

CHIRAZ BOUDJABI

LATMOS, Guyancourt, France

LUCAS BESSON

Météo-France, DSO, Toulouse, and LATMOS, Guyancourt, France

OLIVIER CAUMONT

CNRM-GAME (Météo-France, CNRS), CNRM/GMME/MICADO, Toulouse, France

(Manuscript received and in final form 13 April 2012)

ABSTRACT

Refractivity measurements in the boundary layer by precipitation radar could be useful for convection prediction. Until now such measurements have only been performed by coherent radars, but European weather radars are mostly equipped with noncoherent magnetron transmitters for which the phase and frequency may vary. In this paper, the authors give an analytical expression of the refractivity measurement by a noncoherent drifting-frequency magnetron radar and validate it by comparing with in situ measurements. The main conclusion is that, provided the necessary corrections are applied, the measurement can be successfully performed with a noncoherent radar. The correction factor mainly depends on the local-oscillator frequency variation, which is known perfectly. A second-order error, proportional to the transmitted frequency variation, can be neglected as long as this change remains small.

1. Introduction

Often suggested as a proxy for estimating surface humidity, measurements of refractivity by radar are receiving increasing attention from the meteorological community. The phase variations of the radar ground echoes are related to changes in the refractive index of air between the radar and static targets (Fabry et al. 1997). The refractive index varies with pressure, temperature, and relative humidity, so any phase change is a record of the variation of atmospheric parameters (Demoz et al. 2006; Fritz and Chandrasekar 2009; Wakimoto and Murphey 2010).

For radar equipped with coherent transmitters, the frequency and phase of the pulse are well controlled and these radars can therefore be used to make refractivity measurements. However, most of the operational European radar networks are equipped with noncoherent magnetron transmitters for which phase is unpredictable and frequency can drift over time, and this must be taken into account for Doppler and refractivity measurements.

Nutten et al. (1979) showed that the radial component of the wind could be measured by Doppler shift with a magnetron radar, provided that the phase of every transmitted pulse was measured. As the phase term $4\pi f(t)r/c$ is proportional to the frequency, the use of signal phase also requires that the frequency f should remain sufficiently stable during the measurement time. This can be difficult for refractivity measurements for which we compare the phase of signals separated by long durations (minutes, hours, or days), and corrections must

Corresponding author address: Dr. Jacques Parent du Chatelet, Météo-France, DSO-D, and LATMOS, 11 Bd d'Alembert Guyancourt 78280, France.
E-mail: jacques.parent-du-chatelet@latmos.ipsl.fr

DOI: 10.1175/JTECH-D-12-00070.1

be implemented to take the frequency drifts of the transmitter into account. Another feature to be considered is that the signal frequency on which we perform the measurement is not zero because the signal is the result of mixing between the received signal and the local oscillator, the frequencies of which may be different.

An initial formulation for the phase of a signal backscattered by a static target for a noncoherent magnetron radar has been given by Parent du Chatelet et al. (2007) who conclude that, provided the received signal is sampled exactly at the moment that corresponds to the propagation delay: ''The phase difference between the received signal and the transmitted signal actually only depends on the frequency of the local oscillator, on the distance r and on the refractive index, n,'' and does not depend on the magnetron frequency. The consequences of this result for Doppler and refractivity measurements were considered by Parent du Chatelet and Boudjabi (2008). Junyent et al. (2009) also proposed a correction factor to take the frequency variations of the transmitter into account. In section 2, we develop the formulation of the signal backscattered by a static target for a noncoherent radar, where we pay particular attention to separating the effects due to frequency variations of the local oscillator, frequency variations of the transmitter, and effects due to changes of refractivity between the radar and the target. Finally, we validate the different terms of the theoretical formulation in section 3 with radar data, and we present some preliminary results of radar measurements compared to refractivity values deduced from in situ measurements by Automatic Weather Stations (AWS).

2. Basic equations for refractivity measurement with noncoherent transmitter

Following the formulation of Fabry (2004), the time delay τ_{travel} necessary for the electromagnetic wave to reach a target at distance r and come back to the radar is[1]

$$\tau_{\text{travel}}(r,t) = \frac{2}{c}\int_0^r n(x,t)\,dx = \frac{2r}{c} + \frac{210^{-6}}{c}\int_0^r N(x,t)\,dx, \tag{1}$$

where c is the speed of light in vacuum, $n(x, t)$ is the refractive index, and $N(x, t)$ is the refractivity at distance x and at time t, defined by (Bean and Dutton 1968):

$$N(x,t) = [n(x,t) - 1]10^6. \tag{2}$$

Variations of τ_{travel} due to refractivity changes can only be obtained through phase of the signal, and the purpose of this section is to establish the relationship between signal phase and refractivity changes for a radar whose frequency can vary. The phase depends on the path traveled to the target, and also on transformations in the receiver, which we examine below.

The radar receiver (Fig. 1) has two identical channels for the received signal $S_{\text{RX}}(\tau)$, and for the transmitted signal $S_{\text{TX}}(\tau)$. Both are mixed with the same sinusoidal stable oscillator (STALO) $f_{\text{LO}}(t)$ to provide I and Q zero frequency base-band complex signals $R_{\text{RX}}(\tau)$ for the receive branch and $R_{\text{TX}}(\tau)$ for the transmit branch. A digital AFC unit gives the phase φ_{oT} for each transmitted pulse, and also measures the transmitted frequency $f(t)$. The local oscillator is adjusted to follow the transmitted frequency variations, but the frequency $[f(t) - f_{\text{LO}}(t)]$ of the base-band signal is not exactly zero so that the phase of a signal received from a static isolated target also depends on the sampling time τ_{sam}.

To take account of these points, the following development gives the formulation of the phase $\phi(\tau_{\text{sam}}, t)$ for a signal transmitted at a frequency $f(t)$, backscattered by an isolated remote target located at range r, mixed with a sinusoidal local oscillator of frequency $f_{\text{LO}}(t)$, and sampled at a delay τ_{sam} after transmission. This is schematically illustrated in Fig. 2 where we have represented the shape of the signal before and after the receiver [i.e., before and after multiplication by the local oscillator (LO)].

At the receiver input, the transmitted pulse $S_{\text{TX}}(\tau)$, and the signal $S_{\text{RX}}(\tau)$ received from the target after a delay τ_{travel}, are given by

$$\begin{aligned} S_{\text{TX}}(\tau) &= \cos[2\pi f(t)\tau + \varphi_{0\text{TX}}] \quad \text{for} \quad \tau \in [0, \tau_{\text{pulse}}] \\ S_{\text{RX}}(\tau) &= \text{A}S_{\text{TX}}(\tau - \tau_{\text{travel}}) \\ &= \text{A}\cos[2\pi f(t)(\tau - \tau_{\text{travel}}) + \varphi_{0\text{TX}}] \quad \text{for} \\ \tau &\in [\tau_{\text{travel}}, \tau_{\text{travel}} + \tau_{\text{pulse}}], \end{aligned} \tag{3}$$

where τ_{pulse} is the pulse duration and $\varphi_{0\text{TX}}$ is the transmitted phase. The constant A is for the target amplitude return.

[1] Throughout the paper we use the notation τ for delay after the transmission pulse, and t for time measurement in the sense of minutes or hours. The function $n(x, t)$ is assumed constant during the few radars pulses needed for an individual measurement.

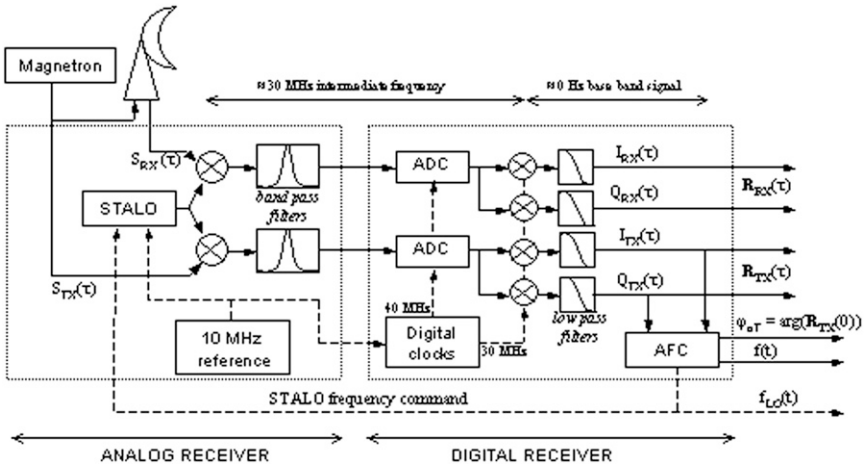

FIG. 1. Simplified diagram of the receiver. It is divided into two channels: one for the ''received signal'' $S_{RX}(\tau)$ and one for the ''transmitted signal'' $S_{TX}(\tau)$. The automatic frequency control (AFC) unit uses the latter channel to measure the frequency $f(t)$ of the transmitted signal and its phase φ_{oT} at time $\tau = 0$. The frequency $f(t)$ is used to command the local oscillator frequency $f_{LO}(t)$. Each of the two channels uses two digital frequency mixers to produce the real and imaginary parts of the two complex received signals $R_{RX}(\tau)$ and $R_{TX}(\tau)$.

At the receiver output, after multiplication by the local oscillator $LO(\tau) = \cos[2\pi f_{LO}(t)\tau - \varphi_{0LO}]$ and low pass filtering, we have the following:

$$
\begin{aligned}
R_{TX}(\tau) &= I_{TX} + jQ_{TX} \\
&= \exp j\{2\pi[f(t) - f_{LO}(t)]\tau + \varphi_{0T}\} \quad \text{for} \\
&\tau \in [0, \tau_{pulse}] \\
R_{RX}(\tau) &= I_{RX} + jQ_{RX} \\
&= A \exp j\{2\pi[f(t)\tau - f_{LO}(t)\tau - f(t)\tau_{travel}] + \varphi_{0T}\} \\
&\text{for} \quad \tau \in [\tau_{travel}, \tau_{travel} + \tau_{pulse}],
\end{aligned}
\tag{4}
$$

where $\varphi_{0T} = \varphi_{0TX} - \varphi_{0LO}$ is the measured transmitted phase for $\tau = 0$.

Here $R_{RX}(\tau)$ is a sinusoidal signal of frequency $[f(t) - f_{LO}(t)]$ and duration τ_{pulse}. The signal is sampled at time τ_{sam}, which is close, but not exactly equal, to τ_{travel}. The measured phase $\phi(\tau_{sam}, t)$ is given by the argument of $R_{RX}(\tau)$ for $\tau = \tau_{sam}$ and, after subtraction of φ_{oT}:

$$
\phi(\tau_{sam}, t) = 2\pi[f(t)\,\tau_{sam} - f(t)\,\tau_{travel} - f_{LO}(t)\,\tau_{sam}]. \tag{5}
$$

Here ϕ, f, f_{LO} and τ_{travel} are all functions of the measurement time t.

To reveal the effects of refractivity variations, which are hidden in τ_{travel}, we define a ''reference refractivity'' N_{ref} as the refractivity in reference conditions of temperature, pressure and humidity. Equation (2) then becomes

$$
n(x,t) = 1 + 10^{-6}N(x,t) = 1 + 10^{-6}[N_{ref} + \delta N(x,t)]. \tag{6}
$$

Using Eqs. (1), (5), and (6), we obtain the following:

$$
\begin{aligned}
&\phi(\tau_{sam}, t) = 2\pi[-f_{LO}(t)\tau_{sam} + f(t)\Delta\tau - f(t)\Delta\tau_N(\tau_{sam}, t)] \quad \text{with} \\
&\Delta\tau = \tau_{sam} - \tau_{travel}(r, t_{ref}) = \tau_{sam} - \frac{2r}{c} - \frac{2r}{c}10^{-6}N_{ref} \quad \text{and} \\
&\Delta\tau_N(\tau_{sam}, t) = \frac{2\times 10^{-6}}{c}\int_0^r \delta N(x,t)\,dx.
\end{aligned}
\tag{7}
$$

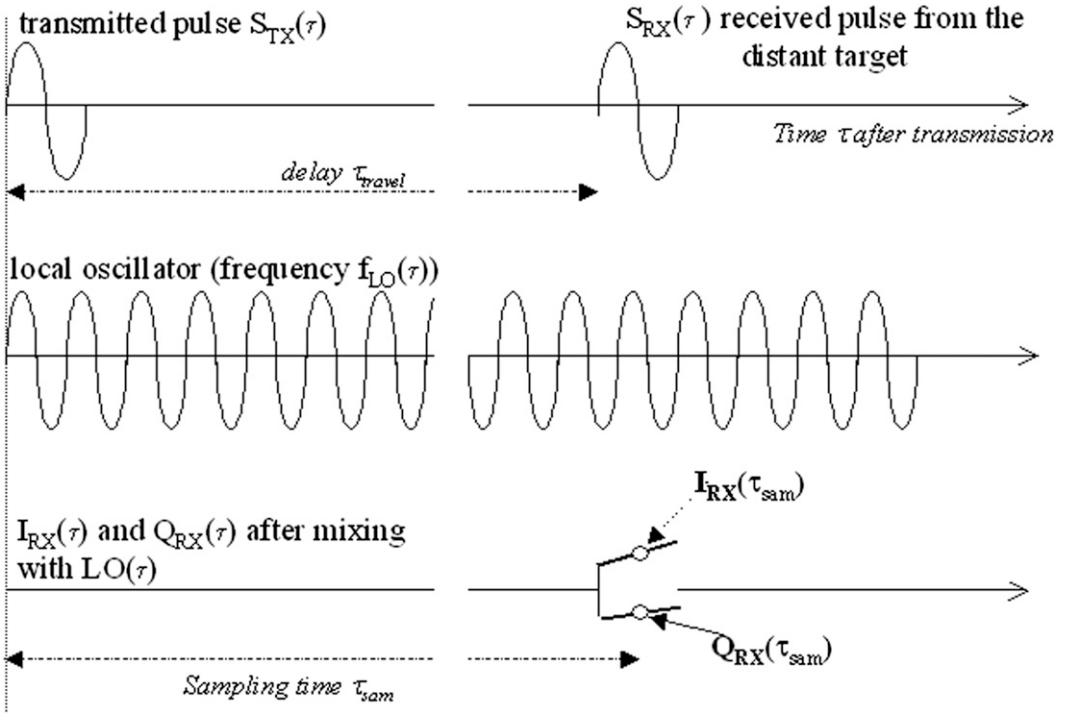

FIG. 2. Schematic diagram of the transmitted pulse $S_{TX}(\tau)$ of duration τ_{pulse} and of a signal $S_{RX}(\tau)$, received from a static isolated remote target. Except for a phase change φ_{target} due to the target and a time delay τ_{travel} due to the propagation, this signal is an exact replica of the transmitted pulse (for simplicity, we assume in the diagram that $\varphi_{target} = 0$). After mixing with the local oscillator, the phase of the signal $R_{RX}(\tau)$ at the exact delay τ_{travel} is equal to the phase of the local oscillator at delay τ_{travel} plus φ_{target}. The variation of $I_{RX}(\tau)$ and $Q_{RX}(\tau)$ within the received pulse (i.e., between τ_{travel} and $\tau_{travel} + \tau_{pulse}$) is due to the difference between the transmitted frequency and the local oscillator frequency. This signal is sampled at the delay τ_{sam}, slightly different from τ_{travel}, and this difference leads to a phase measurement error.

For each pixel, $\Delta\tau$ is a constant equal to the difference (mismatch) between the sampling time and the travel time under reference conditions. Here $\Delta\tau_N(\tau_{sam}, t)$ is the supplementary propagation delay due to the difference of refractivity $\delta N(x, t)$ from the reference conditions. As a consequence $\Delta\tau_N(\tau_{sam}, t_{ref}) = 0$.

Note that, if we consider the particular case of propagation in a vacuum, and if the signal is sampled at the exact delay $2r/c$, then Eq. (7) reduces to $\phi(\tau_{sam}, t) = -4\pi f_{LO}(t)r/c$, which is slightly different from the usual formulation $-4\pi f(t)r/c$: the phase change of the received signal is not exactly proportional to the transmitted frequency, but rather to the frequency of the local oscillator. This unexpected result is easily understandable if we consider that the propagation directly results in a time delay, but does not directly lead to a signal phase shift: strictly speaking, the usual phase change $4\pi f(t)r/c$ is the difference between (i) the received signal phase at the delayed time $2r/c$, and (ii) the reference signal phase at the same delayed time. In the receiver considered here, the reference is the local oscillator, not the transmitted signal.

In Eq. (7), $\phi(\tau_{sam}, t)$ is the sum of three terms, each being the product of a frequency by a time delay, and these three time delays have quite different orders of magnitude: if we assume a largest range of 30 km, a pulse duration of 2 μs, and a maximum refractivity change of 100 units, we have the following: $\tau_{sam} \in [0, 200\ \mu s]$, $\Delta\tau \in [0, 2\ \mu s]$, and $\Delta\tau_N(\tau_{sam}, t) \in [0, 0.02\ \mu s]$.

Starting from Eq. (7), it is straightforward to obtain the expression for the difference $\Delta\phi(\tau_{sam}, t, t_{ref})$ between phases measured at time t and at a reference time t_{ref}, for signals both sampled at the same sampling time τ_{sam}:

$$\Delta\phi(\tau_{sam}, t, t_{ref}) = 2\pi \begin{bmatrix} -[f_{LO}(t) - f_{LO}(t_{ref})]\tau_{sam} \\ +[f(t) - f(t_{ref})]\Delta\tau \\ -f(t_{ref})\Delta\tau_N(\tau_{sam}, t) \end{bmatrix}. \quad (8)$$

In the computation of the third term, we have neglected the phase contribution of $2\pi[f(t_{ref}) - f(t)]\Delta\tau_N(\tau_{sam}, t)$,

TABLE 1. Main technical characteristics of the French Falaise radar (48°55′N, 00°08′W, Normandy region).

Magnetron transmitter wavelength	5 cm (C band, 5.625 GHz)
Peak power	250 kW
Antenna 3-dB beamwidth	1.05°
Azimuthal speed	5° s^{-1}
Elevation angle	0.4°
Transmitted pulses duration	2 μs
Repetition rate	333 s^{-1}
Local oscillators stability	Synthesizer locked by a stable 10^{-8} reference
AFC	Activated only if $\lvert f(t) - f_{LO}(t)\rvert > 70$ kHz

equal to 3.6° for the largest values of $f(t_{ref}) - f(t) =$ 500 kHz and $\Delta\tau_N(\tau_{sam}, t) = 0.02\,\mu$s.

Therefore, the contributions of the variables are now completely separated: $f_{LO}(t)$ alone in the first term, $f(t)$ alone in the second term, and $N(r, t)$ alone in the third term. As in Eq. (7), the phase difference $\Delta\phi$ is the sum of three terms, each of which is the product of a frequency by a time delay:

- The first "local oscillator term" is the product of $[f_{LO}(t) - f_{LO}(t_{ref})]$ by τ_{sam}. A correction is easy to achieve as long as the oscillator frequency $f_{LO}(t)$ is precisely known. An accuracy of 1 (in N units) leads to a phase change of 13° km^{-1} at the C band. Using Eq. (8), a simple computation shows that it corresponds to a relative accuracy of 5×10^{-7} on $f_{LO}(t)$. This can be easily obtained with a synthesizer synchronized by a thermostated reference.
- The second "mismatch term" is the product of $[f(t) - f(t_{ref})]$ by the constant $\Delta\tau$. Using Eqs. (7) and (8), it is straightforward to express the corresponding additive bias ε_N on N estimation:

$$\varepsilon_N = \frac{c10^6}{2r}\frac{f(t) - f(t_{ref})}{f(t_{ref})}\Delta\tau. \qquad (9)$$

For example, for $r = 3$ km, $[f(t) - f(t_{ref})]/f(t_{ref}) = 2\times10^{-5}$ (i.e., a difference of 100 kHz at the C band), and $\Delta\tau = 1\ \mu$s; ε_N scales to unity, which is negligible. This can be different for a higher value of $[f(t) - f(t_{ref})]$ and $\Delta\tau$, or for a lower range integration r.

- The third "refractivity term" is the product of the constant $f(t_{ref})$ *by* $\Delta\tau_N(\tau_{sam}, t)$, which is the difference, between times t and t_{ref}, in the delay produced by the refractivity change from the reference. It is the classical expression of phase versus refractivity change.

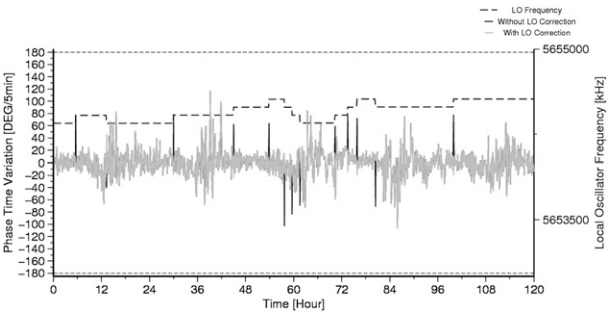

FIG. 3. Time series, during a 5-day period from 3 to 7 Mar 2010, for the signal backscattered by the isolated antenna of the Falaise city's fire station: (i) raw signal 5-min phase change (black line), (ii) same after correction for the local oscillator $f_{LO}(t)$ using Eq. (8) (gray superimposed on the black), and (iii) local oscillator frequency $f_{LO}(t)$ (dashed lines).

3. Initial look at validation by radar and in situ measurements

The experiment was performed with the Falaise radar (see Table 1 for details), part of the French operational network in Normandy, France. Radar measurements have been recorded with a 5-min sampling time, as well as hourly in situ measurements of temperature, pressure, and humidity performed by three AWS within a 30-km radius around the radar. In this study, we specifically process echoes from an isolated mast that is the antenna of the Falaise city fire station, 4.8 km from the radar.

Figure 3 represents the evolution with time of the 5-min phase change during 5 days, from 3 to 7 March 2010. We clearly observe 13 black vertical lines in the 5-min phase change of the raw signal, all of which correspond to local oscillator frequency jumps. These lines are completely suppressed after application of a correction simply deduced from the first term of Eq. (8), which demonstrates its validity.

Many other sharp vertical lines, which are not due to local oscillator frequency changes, can also be observed, particularly during the afternoon (after 12, 36, 60, 84, and 108 h). Previous studies (Besson et al. 2012) have suggested that it is due to diurnal turbulence in the boundary layer, observed between 1300 and 1800 UTC, and generated by the influence of heat radiation on the lowest atmospheric layer, when the sun is at the zenith (Curry et al. 1988).

To identify the phase signature of the second term of Eq. (8), we have compared phases of two signals, both from the isolated fire station target, sampled at two successive range gates τ_{sam1} and τ_{sam2}, separated by 150 m. Using the definition of $\Delta\tau$ by Eq. (7), $[\Delta\tau_2 - \Delta\tau_1]$ in this case is equal to $[\tau_{sam2} - \tau_{sam1}]$, which is perfectly

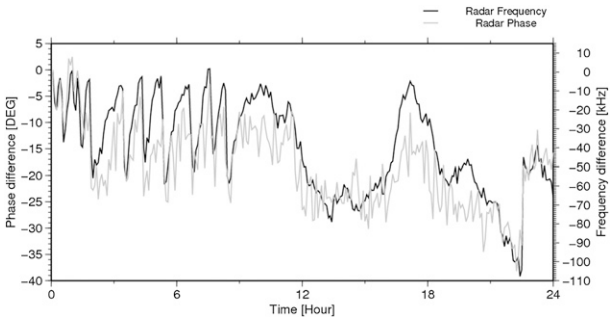

FIG. 4. Time series, for 16 Mar 2010, of the phase difference $\Delta\Phi_{2,1}(t, t_{\text{ref}})$ of two signals coming from the same isolated target sampled at two successive range gates (gray line). The reference time t_{ref} is fixed to the first available time of the day. Time series of the transmitted signal magnetron frequency difference $[f(t) - f(t_{\text{ref}})]$ (black line, right scale in kHz).

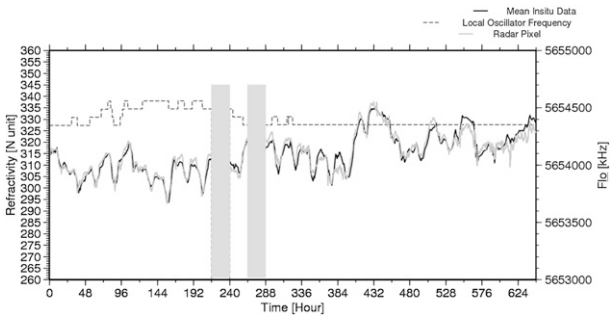

FIG. 5. Time series of refractivity N measured by the radar during a 27-day period (2–30 Mar 2010) for the radar pixel. Averaged refractivity measurements from the three AWS (solid black line). Local oscillator frequency (right scale, dashed line). The two gray columns indicate no data and the time t_{ref} is reset after each period of absence of data.

known. After correction for the local oscillator contribution, Eq. (8) leads here to the expression of the phase difference $\Delta\Phi_{2,1}(t, t_{\text{ref}})$:

$$\Delta\Phi_{2,1}(t, t_{\text{ref}}) = \Delta\Phi(\tau_{\text{sam2}}, t, t_{\text{ref}}) - \Delta\Phi(\tau_{\text{sam1}}, t, t_{\text{ref}}) = 2\pi[f(t) - f(t_{\text{ref}})][\tau_{\text{sam2}} - \tau_{\text{sam1}}]. \quad (10)$$

Figure 4 shows the time variation, during one specific day (16 March 2010) of the frequency change $[f(t) - f(t_{\text{ref}})]$, and the phase change $\Delta\Phi_{2,1}(t, t_{\text{ref}})$. Although differences can be noted here and there, the two curves are nicely correlated ($R^2 = 0.65$) and the main phase changes obviously come from the frequency difference variations $[f(t) - f(t_{\text{ref}})]$. The slope of the linear regression is 0.24° kHz^{-1}, quite close to the expected value of 0.36° kHz^{-1} from Eq. (10). This result proves that the second term of Eq. (8) exists, but a method to estimate $\Delta\tau$ for each pixel remains to be found, in order to be able to correct the errors due to this mismatch term.

We present in Fig. 5 an example of time series of refractivity measured by radar, corrected for the local oscillator changes (gray line) and by in situ AWS (black line). The reference time t_{ref}, initially fixed at the first measurement of the series, is reinitialized after each missing data period (gray vertical bars). The longest time interval without initialization has a 15-day duration, between times 288 and 648 (hours after the begining of the sequence). Radar and in situ measurements compare well, even when significant variations of the local oscillator occur, before time 200. The correlation gives an R^2 coefficient of 0.94 and the slope of the linear regression is equal to 1.0: the two measurements are very close together.

We can therefore conclude that the Eq. (8) formulation is in accordance with radar and in situ measurements. Significant residual problems not shown here have been observed from time to time, but they are actually not due to the nature of the transmitter but more probably to the nature of the target, or to some propagation problem.

4. Summary and conclusions

In this paper, we gave an analytical expression for the phase of a radar signal generated by a noncoherent transmitter and backscattered by a distant static target. This expression leads to three terms:

- the first local oscillator term can be easily corrected;
- the second ''mismatch term'' can be neglected provided that the magnetron frequency variations and the Δt parameter both remain small (100 kHz for the transmitted frequency and 1 μs for $\Delta\tau$);
- the third refractivity term, which connects the signal phase to the refractivity.

This confirms the conclusion of Parent du Chatelet et al. (2007) that the received signal phase depends much more on the local oscillator frequency than on that of the transmitted frequency. These two frequencies can be different with magnetron-transmitter radars.

The analytical expression has been validated by experimental radar measurements compared with in situ measurements by AWS. The conclusion is that refractivity measurements can be performed with noncoherent radars as well as with coherent radars, providing that the local oscillator frequency is precisely defined (10^{-8} is accurate enough), and that a correction is applied for the frequency variations of the local oscillator.

In the future, we will use this tool to validate a measurement strategy adapted to our context, and based on the previous studies by Fabry (2004). After that, the method will be deployed in the French ''Application

Radar à la Météorologie Infra-Synoptique'' (ARAMIS) operational radar network to produce refractivity measurements for assimilation by numerical weather prediction systems.

Acknowledgments. The authors thank the directors of Météo-France/DSO and Météo-France/CNRM for having supported this work. They also thank the technicians and engineers from the Centre de Météorologie Radar for their help in obtaining data from the Falaise radar, particularly Laurent Perier.

REFERENCES

Bean, B. R., and E. J. Dutton, 1968: *Ratio Meteorology. National Bureau of Standards Monogr.,* No. 92, National Bureau Standards, 435 pp.

Besson, L., C. Boudjabi, O. Caumont, and J. Parent du Chatelet, 2012: Links between weather phenomena and characterictics of refractivity measured by precipitation radar. *Bound.-Layer Meteor.,* **143,** 77–95, doi:10.1007/s10546-011-9656-7.

Curry, J. A., E. E. Ebert, and G. F. Herman, 1988: Mean and turbulence structure of the summertime arctic cloudy boundary layer. *Quart. J. Roy. Meteor. Soc.,* **114,** 715–746.

Demoz, B., and Coauthors, 2006: The dry line on 22 May 2002 during IHOP 2002: Convective-scale measurements at the profiling site. *Mon. Wea. Rev.,* **134,** 294–310.

Fabry, F., 2004: Meteorological value of ground target measurements by radar. *J. Atmos. Oceanic Technol.,* **21,** 560–573.

——, C. Frush, I. Zavadski, and A. Kilambi, 1997: On the extraction of near surface index of refractivity using radar phase measurements from ground targets. *J. Atmos. Oceanic Technol.,* **14,** 978–987.

Fritz, J., and V. Chandrasekar, 2009: Implementation and analysis of networked radar refractivity retrieval. *J. Atmos. Oceanic Technol.,* **26,** 2123–2135.

Junyent, F., V. Chandrasekar, and N. Bharadwaj, 2009: Uncertainties in phase and frequency estimation with a magnetron radar: Implication for clear air measurements. *Proc. IGARSS 2009 Conf.,* IGARSS, 613–616.

Nutten B., P. Amayenc, M. Chong, D. Hauser, F. Roux, and J. Testud, 1979: The RONSARD radars: A versatile C-Band dual Doppler facility. *IEEE Trans. Geosci. Electron.,* **GE-174,** 281–288.

Parent du Chatelet, J., and C. Boudjabi, 2008: A new formulation for signal reflected from a target using a magnetron radar. Consequences for Doppler and refractivity measurements. *Extended Abstracts, Fifth European Conf. on Radar in Meteorology and Hydrology,* Helsinki, Finland, FMI, 0166.

——, P. Tabary, and C. Boudjabi, 2007: Evaluation of the refractivity measurement feasibility with a C band radar equipped with a magnetron transmitter. Preprints, *33rd Conf. on Radar Meteorology,* Cairns, Australia, Amer. Meteor. Soc., 8B.6. [Available online at https://ams.confex.com/ams/33Radar/techprogram/paper_123581.htm.]

Wakimoto, R. M., and H. V. Murphey, 2010: Frontal and radar refractivity analyses of the dryline on 11 June 2002 during IHOP. *Mon. Wea. Rev.,* **138,** 228–240.